Supplementary Material

Enhanced selectivity towards melanoma cells with zinc(II)-Schiff bases containing imidazole derivatives

Leonor Côrte-Real[a], Baris Sergi[b]†, Busra Yildirim[b]†, Raquel Colucas[a], Radosław Starosta[a,c], Xavier Fontrodona[d], Isabel Romero[d], Vânia André[a], Ceyda Acilan[b,e]*, Isabel Correia[a]*

[a]Centro de Química Estrutural, Institute of Molecular Sciences, and Department of Chemical Engineering, Instituto Superior Técnico, Universidade de Lisboa, Avenida Rovisco Pais, 1049-001 Lisboa, Portugal

[b]Koç University, School of Medicine, Sariyer, Istanbul, Turkey

[c]Faculty of Chemistry, University of Wrocław, ul. F. Joliot-Curie 14, 50-383 Wrocław, Poland

[d]Departament de Química and Serveis Técnicas de Recerca, Universitat de Girona, Spain

[e]Koç University, Research Center for Translational Medicine (KUTTAM), Istanbul, Turkey

*Correspondence: icorreia@tecnico.ulisboa.pt and cayhan@ku.edu.tr
†These authors contributed equally to this work.

Table S1. ESI-MS characterization of the ligand precursors and corresponding metal complexes in positive mode.

Compound	Species	Calc (*m/z*)	Found (*m/z*)
HL^1	$[M+H]^+$	281.14	281.18
	$[M+K]^+$	319.09	319.10
	$[2M+H]^+$	561.27	561.10
	$[2M+K]^+$	599.22	598.95
HL^2	$[M+H]^+$	295.16	295.20
	$[M+K]^+$	333.11	333.10
	$[2M+H]^+$	589.31	589.09
	$[2M+K]^+$	627.26	626.98
Zn(L^1)$_2$	$[M+H]^+$	623.19	623.07
	$[M+Na]^+$	645.17	645.19
Zn(L^2)$_2$	$[M+H]^+$	651.22	651.12
	$[M+Na]^+$	673.20	673.15

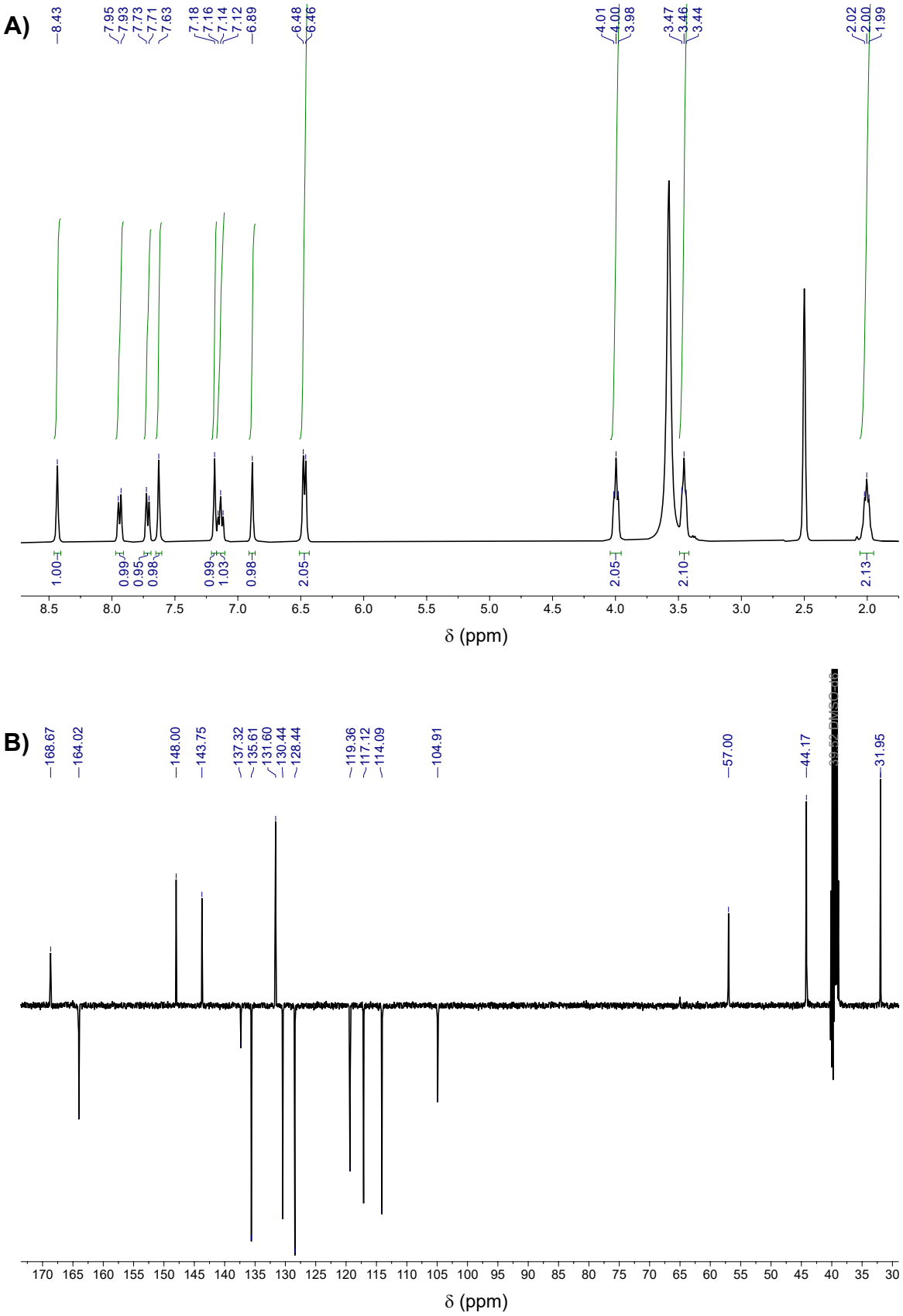

Figure S1. ^{1}H (400 MHz, **A**) and APT-$^{13}C\{^{1}H\}$ (100 MHz, **B**) NMR spectra of ligand **HL¹** in DMSO-d^6 at 298 K.

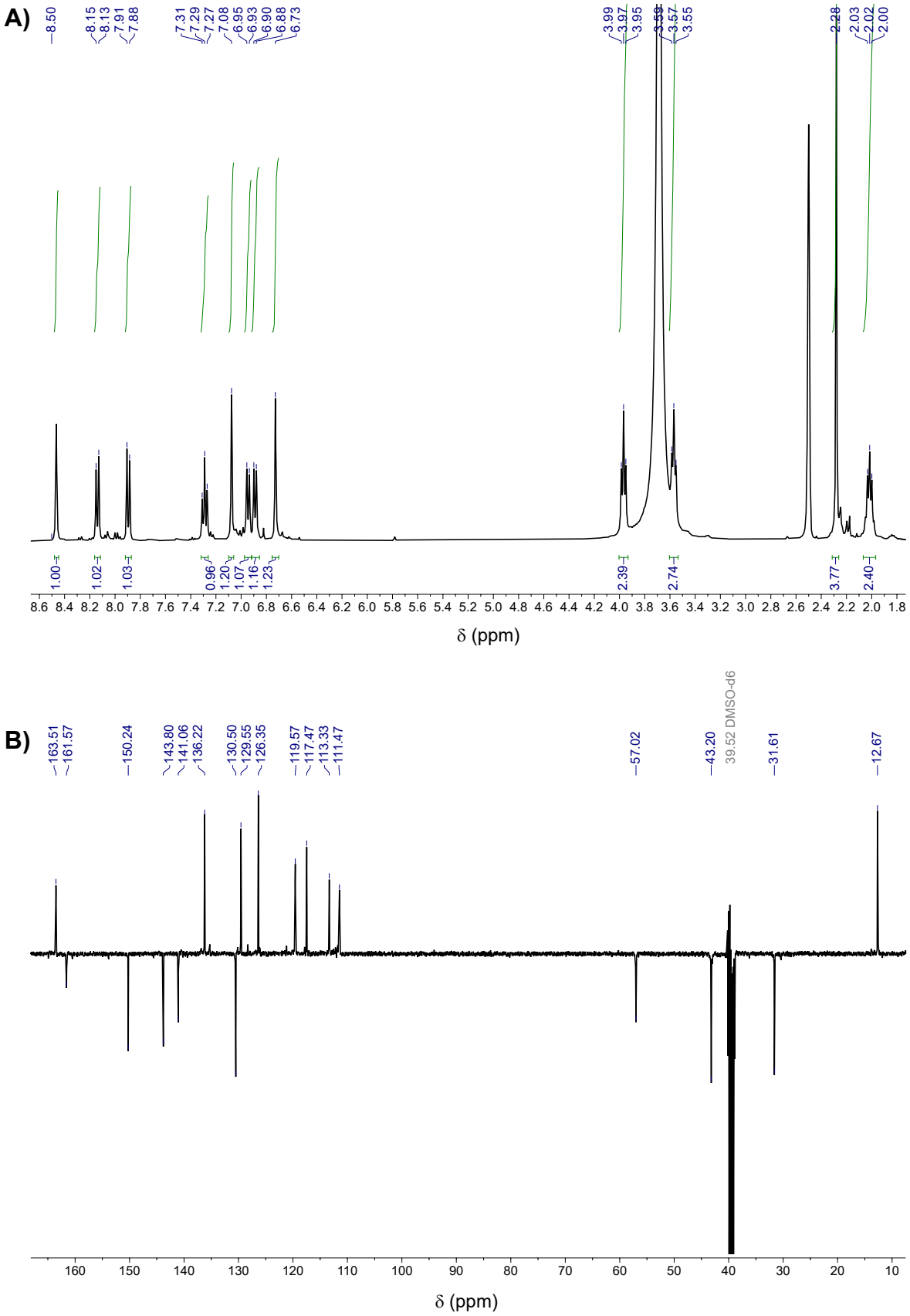

Figure S2. ^{1}H (400 MHz, **A**) and APT-$^{13}C\{^{1}H\}$ (100 MHz, **B**) NMR spectra of ligand **HL²** in DMSO-d^6 at 298 K.

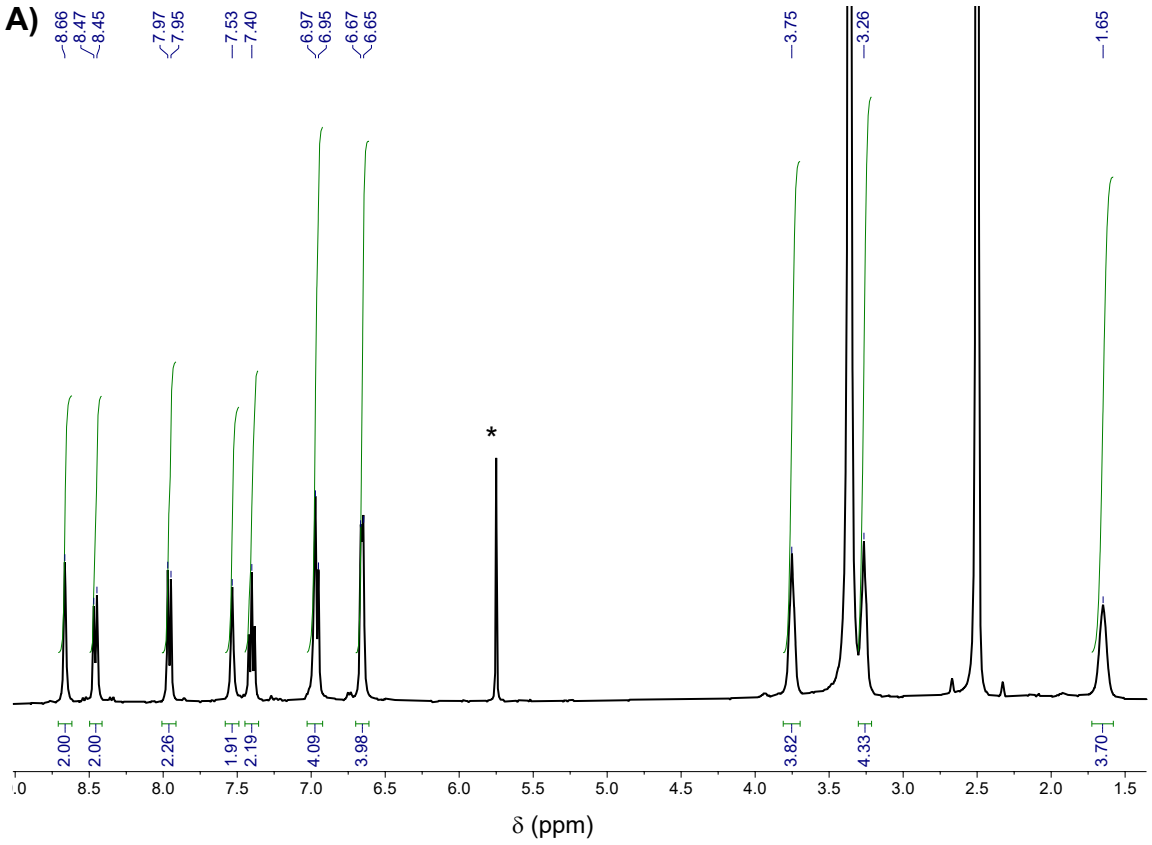

*Residual peak of dichloromethane

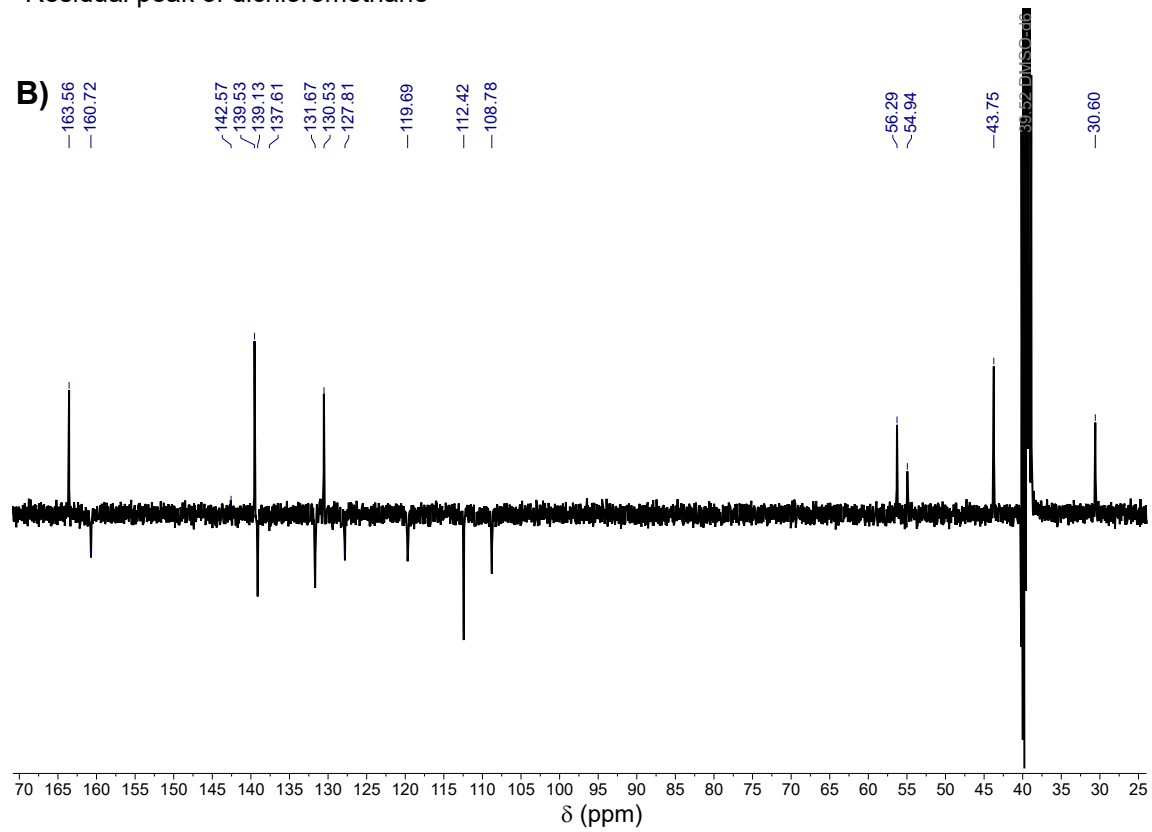

Figure S3. ^{1}H (400 MHz, **A**) and APT-^{13}C{^{1}H} (100 MHz, **B**) NMR spectra of complex **Zn(L^{1})$_2$** in DMSO-d^6 at 298 K.

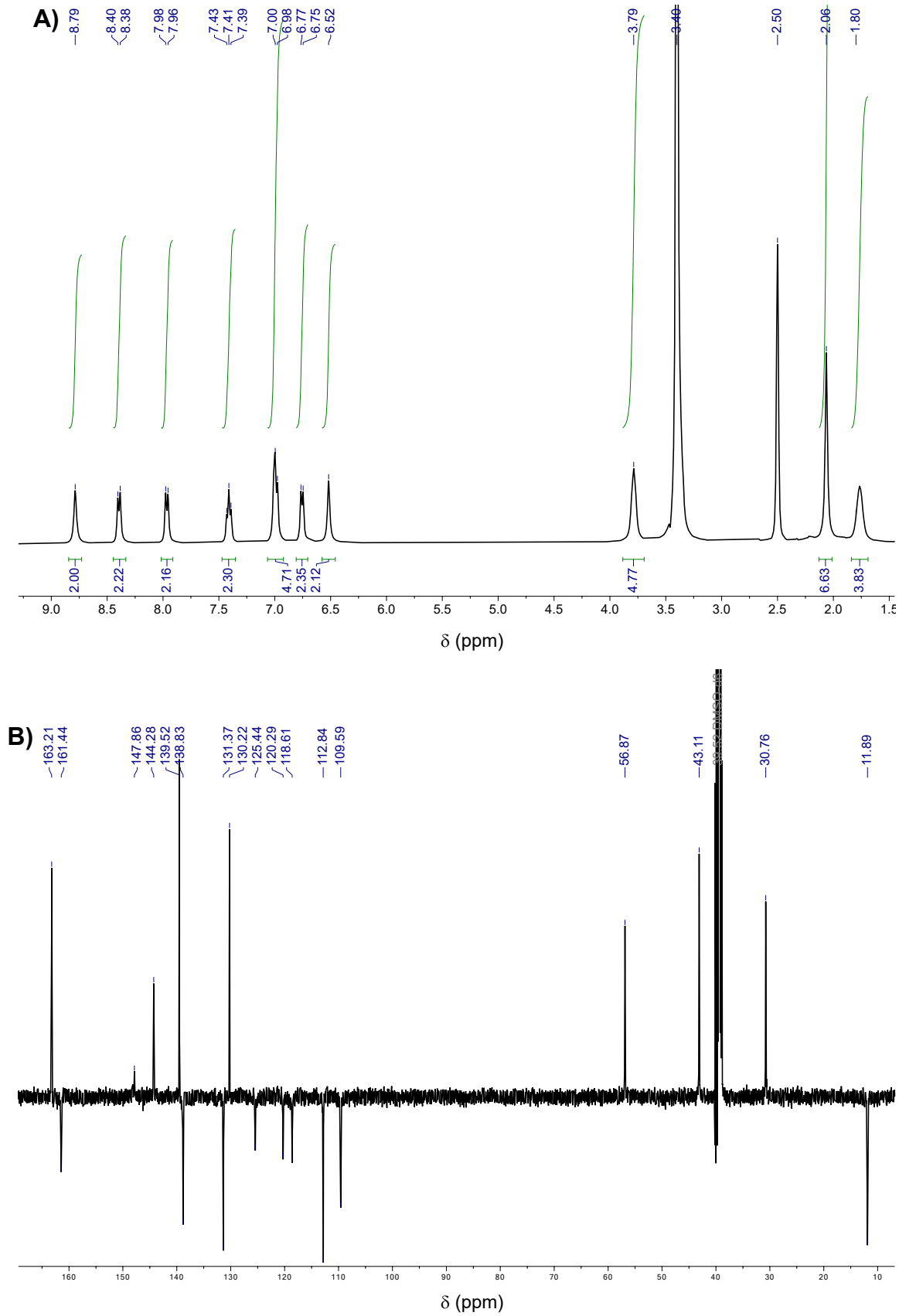

Figure S4. ^{1}H (400 MHz, **A**) and APT-$^{13}C\{^{1}H\}$ (100 MHz, **B**) NMR spectra of complex **Zn(L²)₂** in DMSO-d⁶ at 298 K.

Table S2. Optical spectral data for ligands **HL¹** and **HL²** and their respective Zn(II)-complexes in dichloromethane and DMSO. Measurements were performed at room temperature using 10^{-4}–10^{-6} M solutions. (sh = shoulder).

	λ_{max} /nm (ε x 10^3 / $M^{-1}cm^{-1}$)	
	Dichloromethane	**Dimethylsulfoxide**
HL¹	-	315 (sh), 351 (1.95)
HL²	-	314 (sh), 351 (1.87)
$Zn(L^1)_2$	269 (sh), 300 (50.57), 349 (sh), 371 (sh), 453 (sh), 492 (2.70)	269 (26.62), 298 (45.64), 344 (sh), 367 (sh), 488 (2.65)
$Zn(L^2)_2$	292 (43.29), 310 (sh), 350 (sh), 372 (sh), 439 (2.5), 523 (sh)	268 (29.13), 296 (38.43), 349 (sh), 371 (sh), 468 (2.04), 514 (sh)

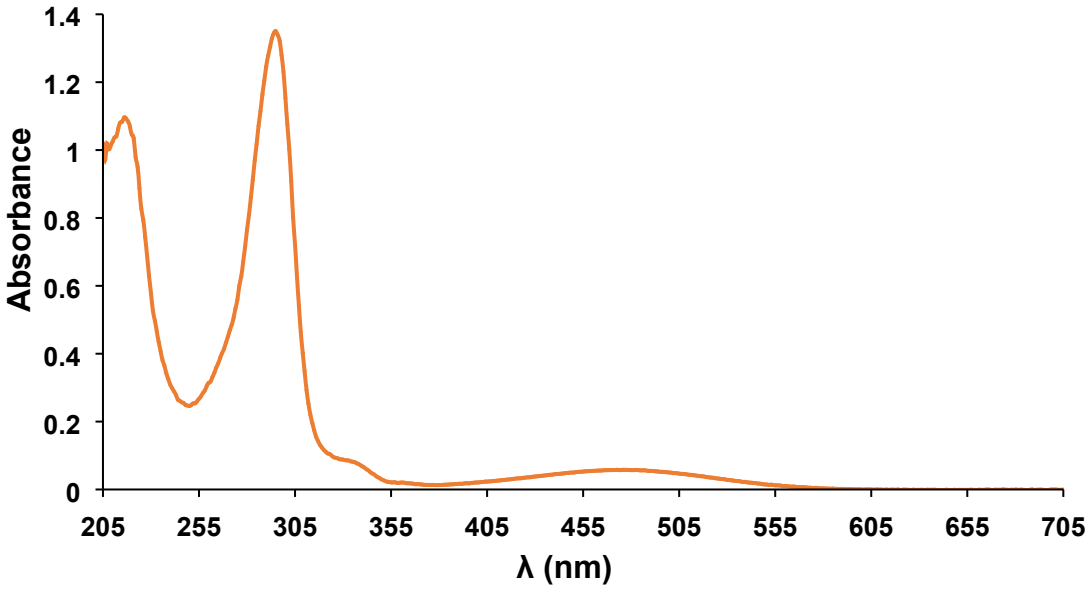

Figure S5. UV-vis absorbance spectra of **$Zn(L^1)_2$** measured in MeOH (25 μM).

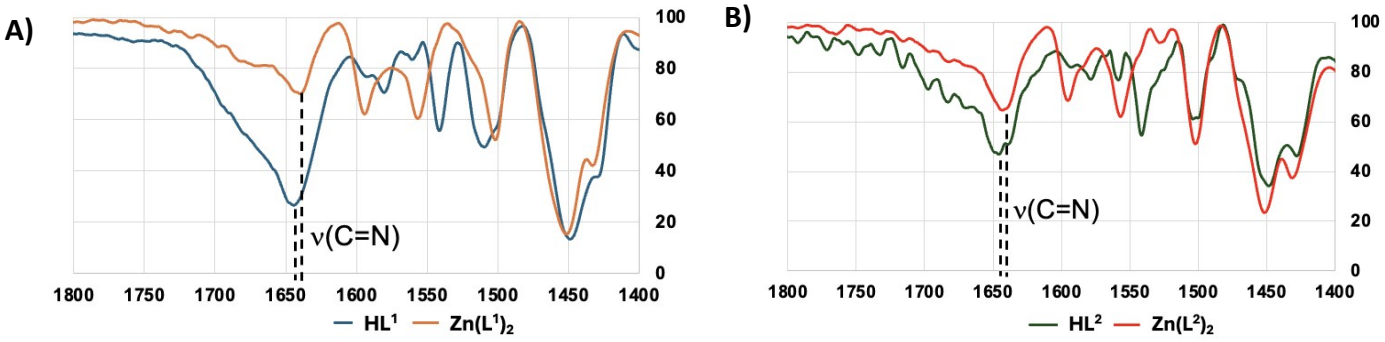

Figure S6. FTIR spectral difference of the azomethine group band frequencies between the free ligands and complexes. **A) HL¹** *vs* **Zn(L¹)₂** and **B) HL²** *vs* **Zn(L²)₂**.

Table S3. Bond lengths (Å) and angles (°) for **HL²**.

O(1)-C(8)	1.344(3)	N(1)-C(2)	1.319(3)
N(1)-C(9)	1.377(3)	N(3)-C(17)	1.357(3)
N(3)-C(15)	1.381(3)	N(3)-C(14)	1.472(3)
N(4)-C(17)	1.326(3)	N(4)-C(16)	1.382(3)
N(2)-C(11)	1.267(3)	N(2)-C(12)	1.463(3)
C(2)-C(3)	1.410(3)	C(2)-C(11)	1.476(3)
C(9)-C(10)	1.416(3)	C(9)-C(8)	1.431(3)
C(10)-C(5)	1.408(3)	C(10)-C(4)	1.420(3)
C(8)-C(7)	1.373(3)	C(17)-C(18)	1.486(3)
C(16)-C(15)	1.353(3)	C(4)-C(3)	1.356(3)
C(5)-C(6)	1.366(3)	C(13)-C(14)	1.506(3)
C(13)-C(12)	1.524(3)	C(6)-C(7)	1.404(3)
C(2)-N(1)-C(9)	117.74(19)	C(17)-N(3)-C(15)	107.30(19)
C(17)-N(3)-C(14)	125.68(19)	C(15)-N(3)-C(14)	126.98(19)
C(17)-N(4)-C(16)	105.88(19)	C(11)-N(2)-C(12)	115.5(2)
N(1)-C(2)-C(3)	123.7(2)	N(1)-C(2)-C(11)	115.4(2)
C(3)-C(2)-C(11)	121.0(2)	N(1)-C(9)-C(10)	122.3(2)
N(1)-C(9)-C(8)	118.5(2)	C(10)-C(9)-C(8)	119.2(2)
C(5)-C(10)-C(9)	120.1(2)	C(5)-C(10)-C(4)	122.5(2)
C(9)-C(10)-C(4)	117.4(2)	O(1)-C(8)-C(7)	124.0(2)
O(1)-C(8)-C(9)	117.18(19)	C(7)-C(8)-C(9)	118.8(2)
N(4)-C(17)-N(3)	110.7(2)	N(4)-C(17)-C(18)	125.6(2)
N(3)-C(17)-C(18)	123.6(2)	C(15)-C(16)-N(4)	109.9(2)
C(3)-C(4)-C(10)	119.6(2)	C(4)-C(3)-C(2)	119.3(2)
N(2)-C(11)-C(2)	123.0(2)	C(16)-C(15)-N(3)	106.2(2)
C(6)-C(5)-C(10)	119.5(2)	C(14)-C(13)-C(12)	112.3(2)
C(5)-C(6)-C(7)	121.1(2)	C(8)-C(7)-C(6)	121.2(2)
N(3)-C(14)-C(13)	112.74(19)	N(2)-C(12)-C(13)	111.4(2)

Table S4. Hydrogen bond details for **HL²**.

Symmetry Operation	**D–H···A**	***d*(D-H) (Å)**	***d*(H···A) (Å)**	***d*(D···A) (Å)**	**(DHA) (°)**
1+x, y, -1+ z	O_1–H_{01}···N_4	0.82	1.89	2.6691(8)	169

Table S5 - Selected bond lengths (Å) and angles (°) for of the 1D $[\mathbf{Zn(L^1)_2]_n}$ polymer.

Zn(1)-N(4)	2.143(4)
Zn(1)-O(1)	2.058(3)
Zn(1)-N(1)	2.254(4)
N(2)-C(11)	1.272(4)
N(2)-C(12)	1.457(5)
N(3)-C(14)	1.461(4)
N(3)-C(15)	1.362(4)
N(3)-C(17)	1.340(4)
O(1)-Zn(1)-O(1)	180
N(4)-Zn(1)-O(1)	89.08(16)
N(4)-Zn(1)-O(1)	90.92(16)
N(4)-Zn(1)-N(4)	180.00(11)
O(1)-Zn(1)-N(1)	78.13(12)
O(1)-Zn(1)-N(1)	101.87(12)
N(4)-Zn(1)-N(1)	92.06(13)
N(4)-Zn(1)-N(1)	87.94(13)
N(1)-Zn(1)-N(1)	180

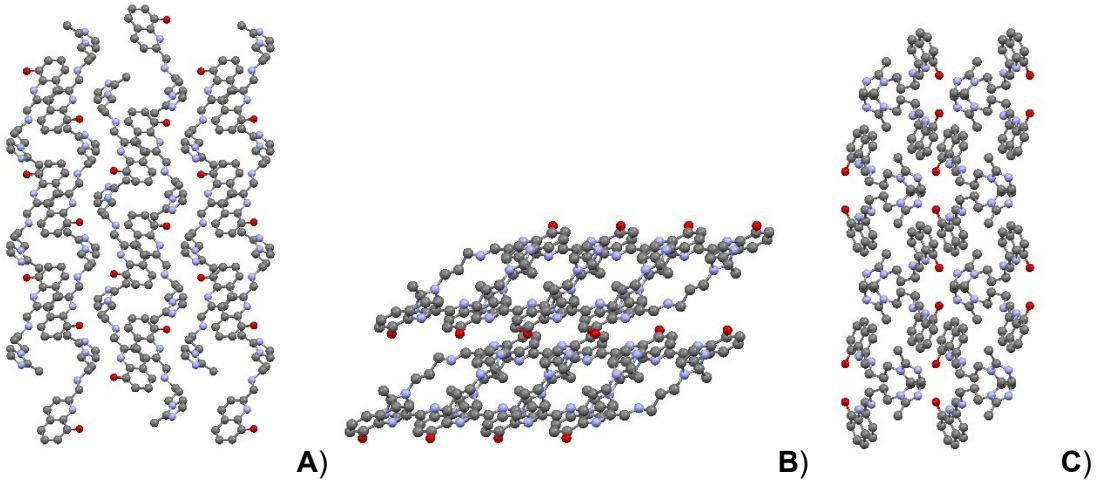

Figure S7. Supramolecular arrangement of **HL²**, in views along the (**A**) *a*, (**B**) *b*, and (**C**) *c* axis. Hydrogen atoms have been omitted for clarity.

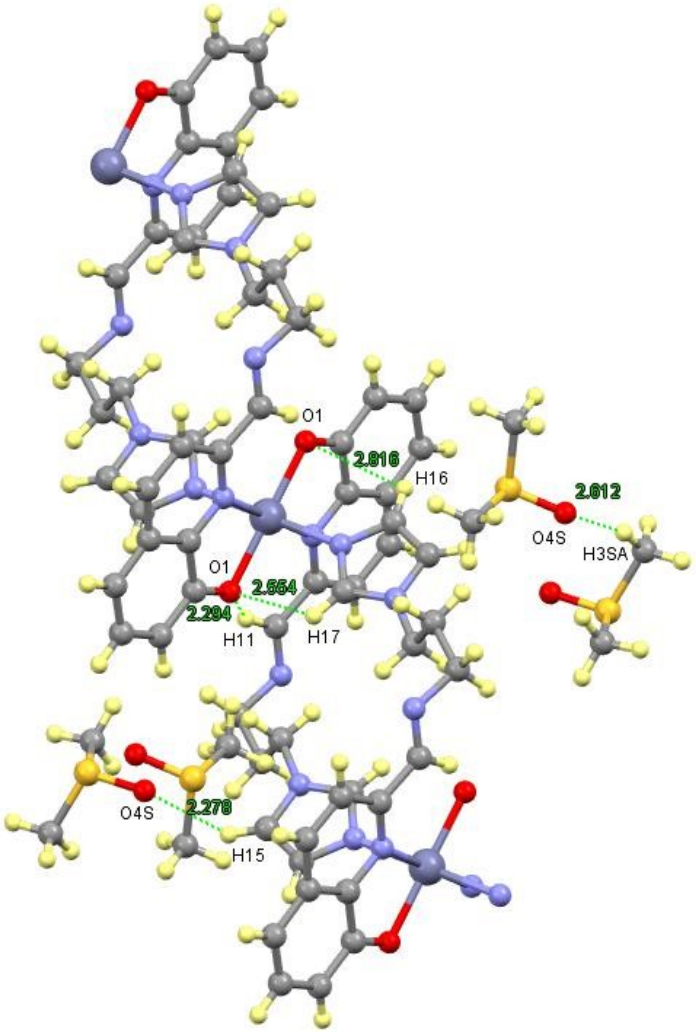

Figure S8. Intra- and intermolecular hydrogen bonds of $[Zn(L^1)_2]_n$.

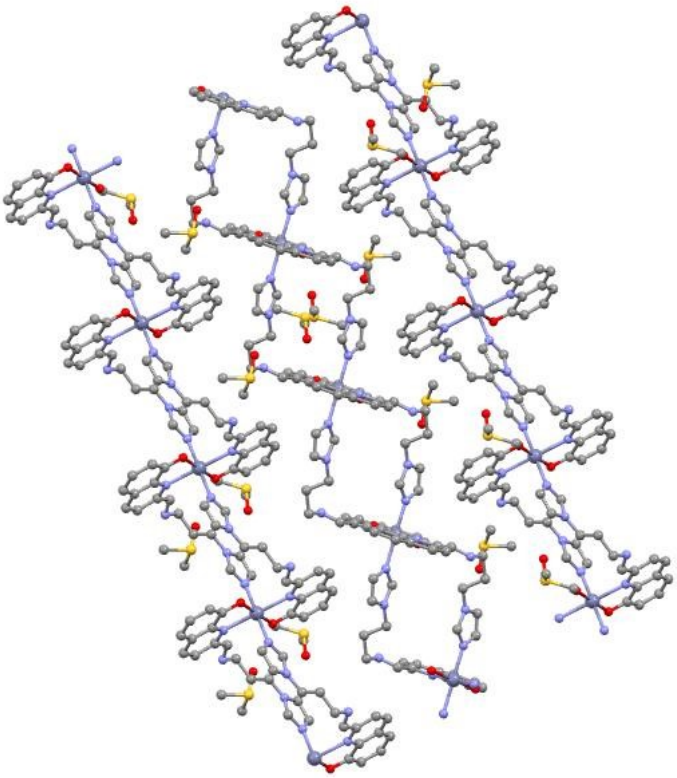

Figure S9. Supramolecular structure of the polymer $\mathbf{[Zn(L^1)_2]_n}$.

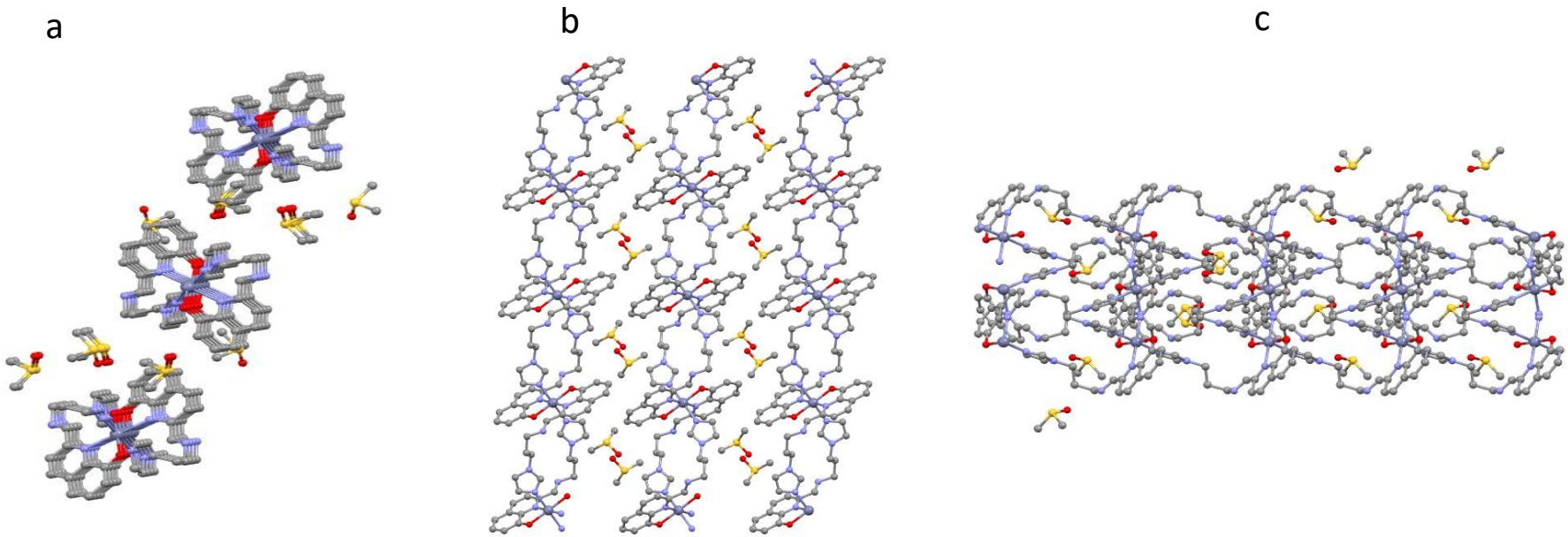

Figure S10. Packing of **$[Zn(L^1)_2]_n$** along the **a)** a axis, **b)** b axis and **c)** c axis.

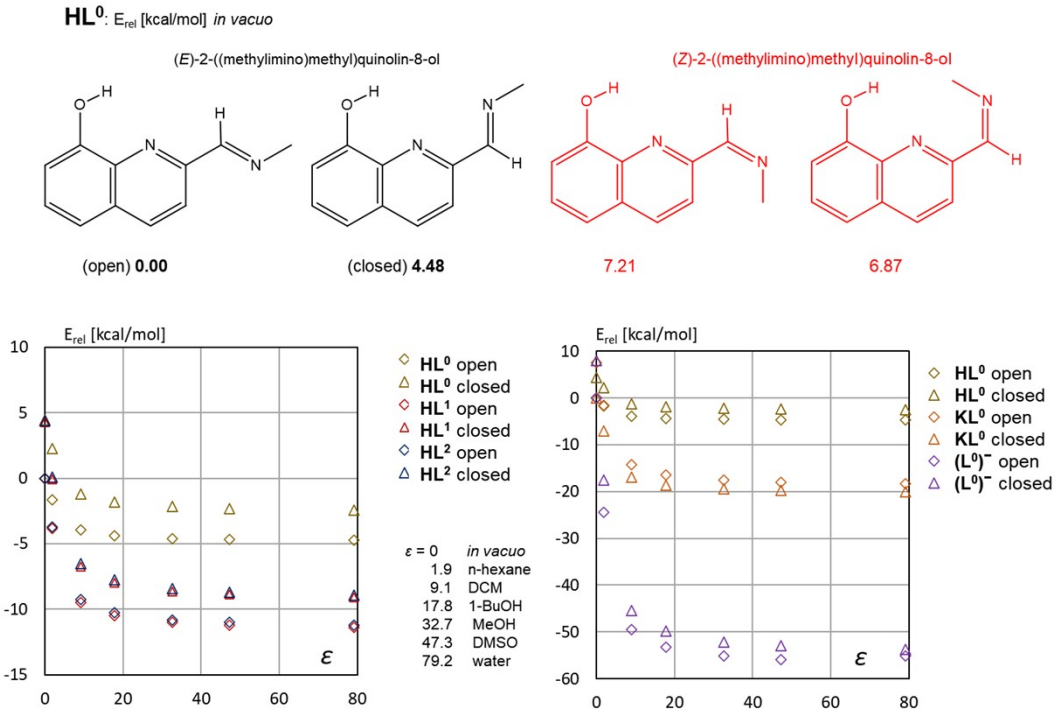

Figure S11. (TOP) 4 conformers of the **HL⁰** ligand (2-((methylimino)methyl)quinolin-8-ol) – relative energies (kcal/mol) calculated *in vacuo*. (BOTTOM) relative energies of two lower energy isomers of **HL⁰**, **HL¹** and **HL²** together with anionic $(\mathbf{L^0})^-$ and the potassium complex **KL⁰** in different solvents (PCM model).

Table S6. Relative energies (kcal/mol) of two lowest energy isomers of **HL⁰**, **HL¹** and **HL²** together with anionic $(\mathbf{L^0})^-$, **KL⁰**, and **Zn(L⁰)Cl** in different solvents (PCM model).

	solvent	ε	E_{rel} [kcal/mol]					
			HL⁰	**HL¹**	**HL²**	**$(L^0)^-$**	**KL⁰**	**Zn(L⁰)Cl**
open	*in vacuo*	*0*	**0**	**0**	**0**	**0**	7.59	0.25
	n-hexane	1.89	-1.63	-3.84	-3.73	-24.44	-1.47	-5.73
	DCM	9.1	-3.96	-9.46	-9.27	-49.46	-14.17	-16.04
	1-BuOH	17.8	-4.37	-10.46	-10.28	-53.21	-16.38	-18.16
	MeOH	32.7	-4.59	-11.00	-10.82	-55.15	-17.58	-19.33
	DMSO	47.29	-4.66	-11.19	-11.01	-55.83	-17.99	-19.75
	water	79.2	-4.73	-11.37	-11.19	-55.15	-18.38	-20.16
closed	*in vacuo*	*0*	4.48	4.31	4.38	8.05	**0**	**0**
	n-hexane	1.89	2.27	-0.07	0.10	-17.53	-7.02	-6.61
	DCM	9.1	-1.17	-6.73	-6.51	-45.36	-16.85	-18.08
	1-BuOH	17.8	-1.82	-7.97	-7.75	-49.80	-18.56	-20.34
	MeOH	32.7	-2.17	-8.64	-8.43	-52.14	-19.46	-21.48
	DMSO	47.29	-2.29	-8.88	-8.67	-52.97	-19.78	-22.02
	water	79.2	-2.41	-9.11	-8.90	-53.74	-20.08	-22.38

Table S7. Relative energies (kcal/mol) of three isomers of **Zn(L^0)$_2$** in different solvents (PCM model).

	solvent	ε	E_{rel}		
			- cc	**- co**	**- oo**
Zn(L^0)$_2$	*in vacuo*	*0*	**0**	1.67	2.60
	n-hexane	1.89	-4.85	-3.15	-2.02
	DCM	9.1	-13.21	-10.90	-9.55
	1-BuOH	17.8	-14.96	-12.41	-11.04
	MeOH	32.7	-15.93	-13.25	-11.88
	DMSO	47.29	-16.29	-13.55	-12.18
	water	79.2	-16.63	-13.84	-12.46

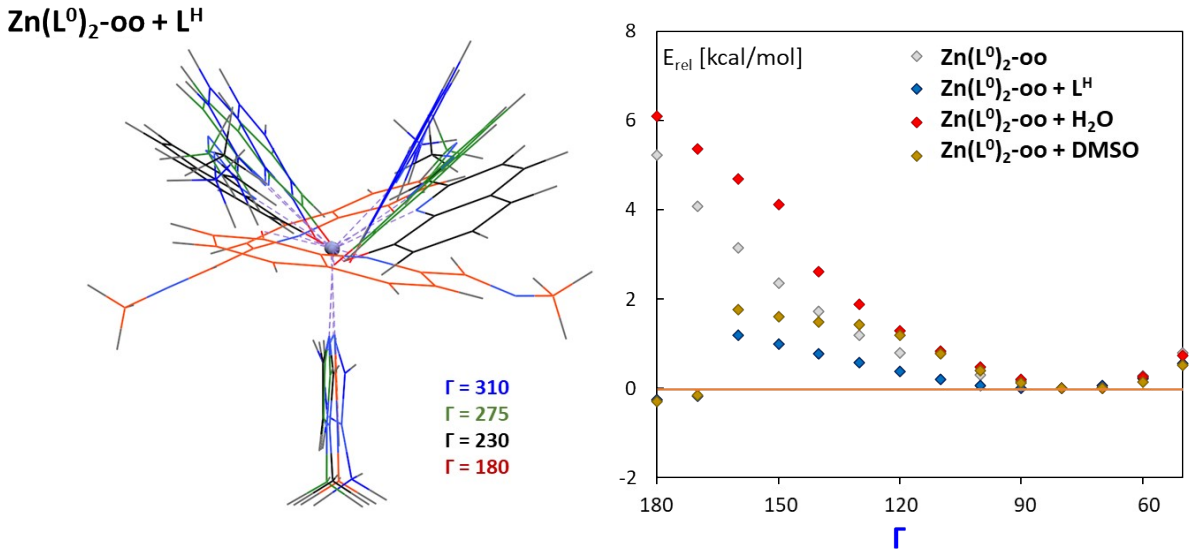

Figure S12. The conformers of the **Zn(L^0)$_2$-oo** isomer in vacuo in the presence of different ligands: H_2O, DMSO, and 1-methyl-1*H*-imidazole (**L^H**) (Γ - the C(8)-O-O-C(8) torsional angle)

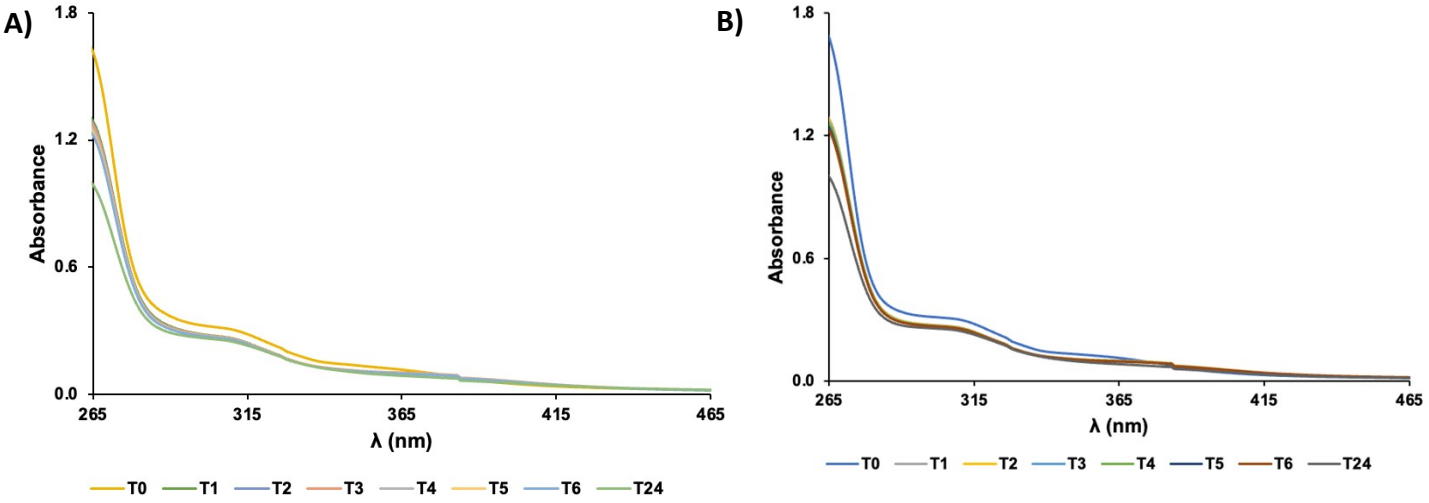

Figure S13. UV-Vis spectra of **A**) **HL¹** (65 μM) and **B**) **HL²** (81 μM) from time zero to the 24 h measurement in HEPES buffer (10 mM, pH 7.4) with 5% (v/v) DMSO.

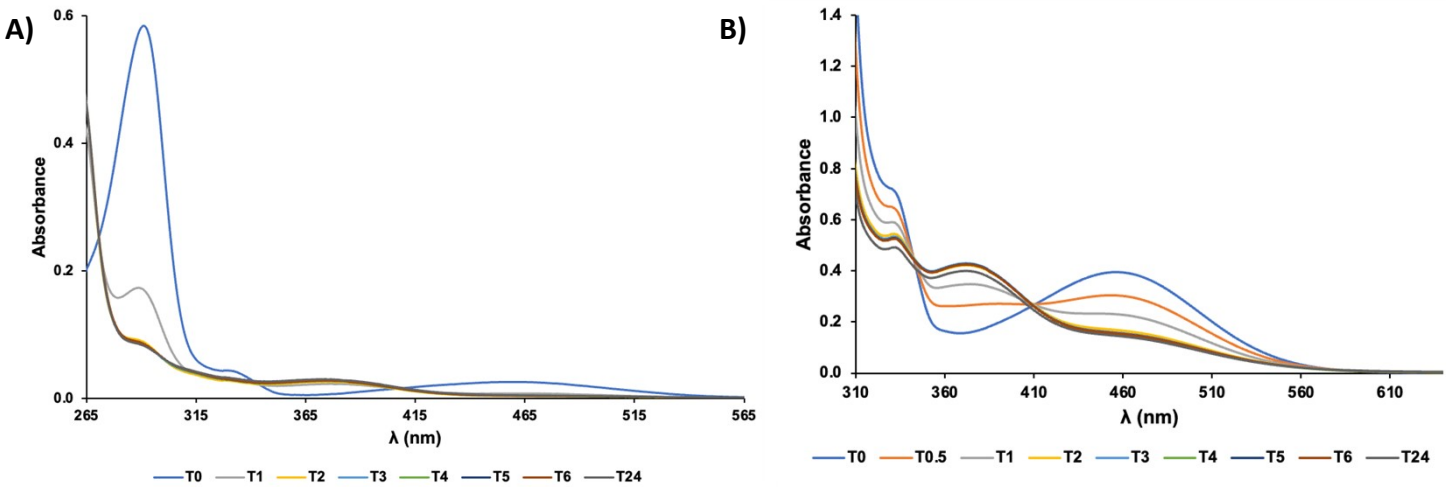

Figure S14. UV-Vis spectra of **A**) **Zn(L¹)$_2$**, 10 μM and **B**) 160 μM – **B**, from time zero to the 24 h measurement in HEPES buffer (10 mM, pH 7.4) with 5% (v/v) DMSO.

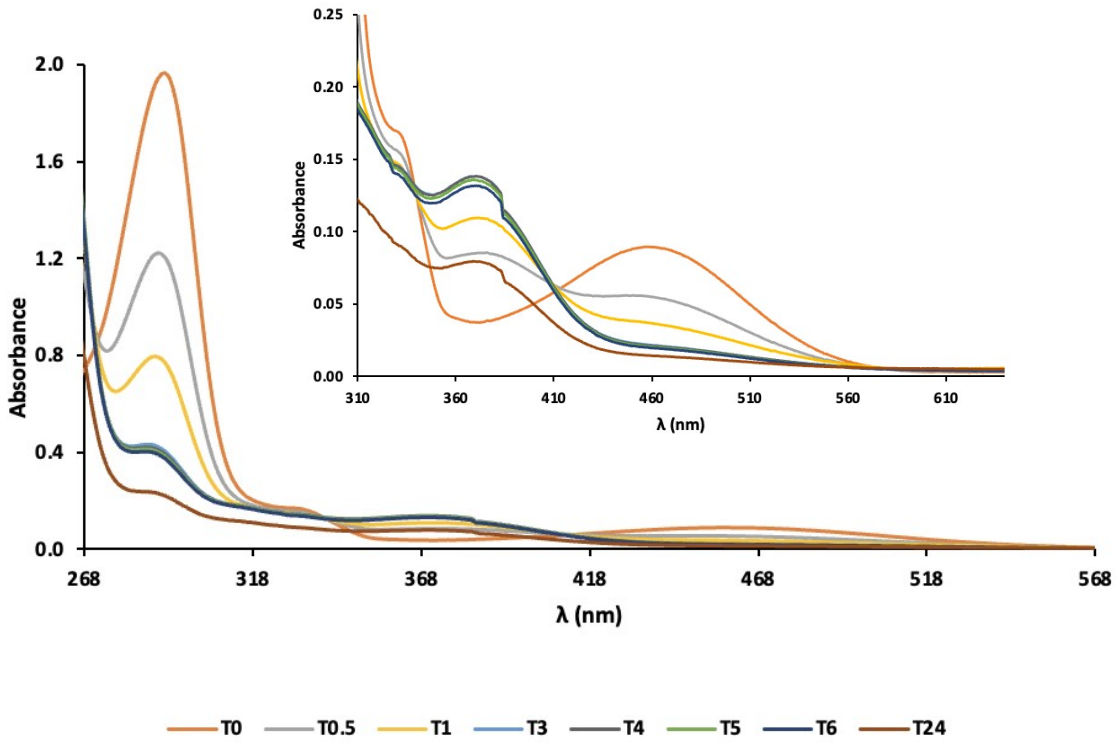

Figure S15. UV-Vis spectra of **Zn(L²)₂**, at 50 μM, from time zero to the 24 h measurement in HEPES buffer (10 mM, pH 7.4) with 5% (v/v) DMSO. Inset – expansion of the spectra at the CT region.

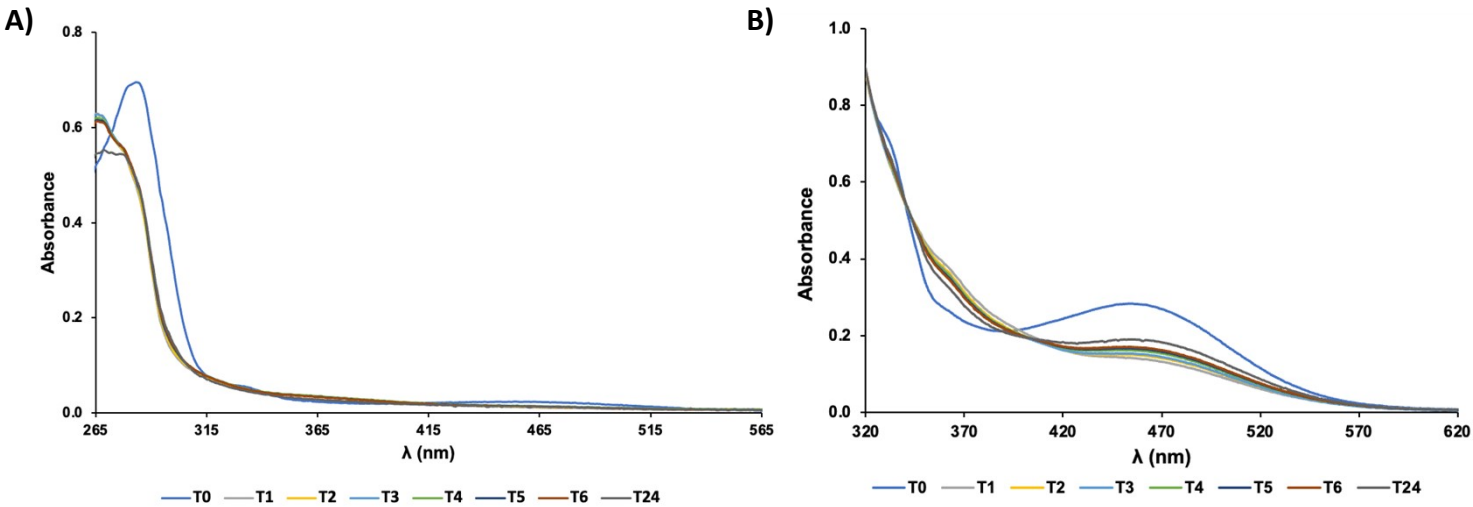

Figure S16. UV-Vis spectra of **A**) **Zn(L¹)₂**, 10 μM and **B**) 160 μM, from time zero to the 24 h measurement in HEPES buffer (10 mM, pH 7.4) with 5% (v/v) DMSO, in the presence of BSA in a 1:1 ratio.

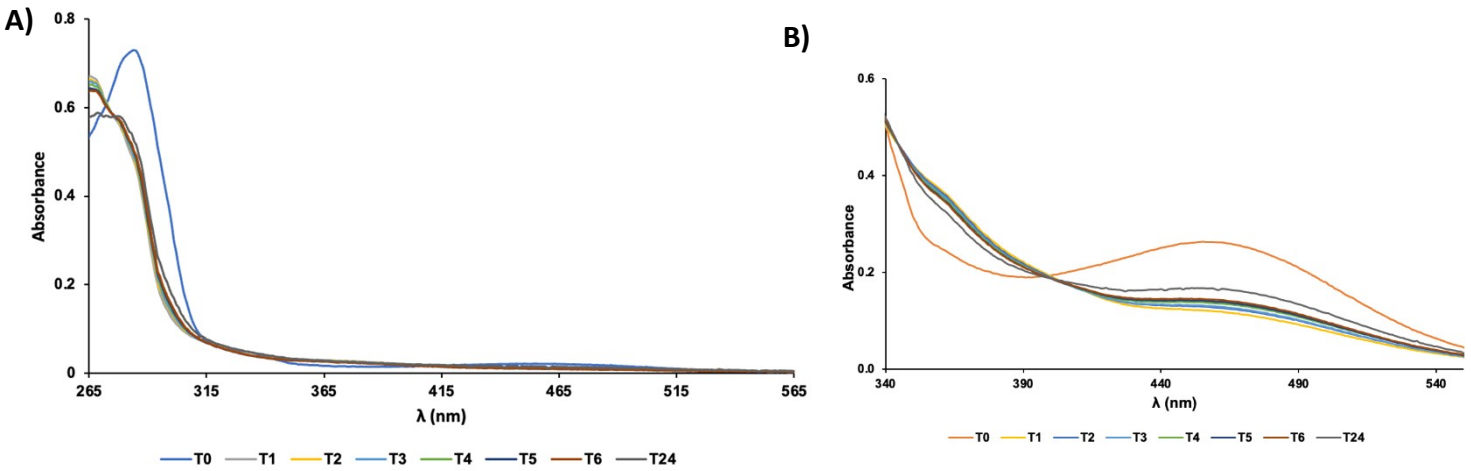

Figure S17. UV-Vis spectra of **A**) **Zn(L^2)$_2$**, 10 μM and **B**) 160 μM, from time zero to the 24 h measurement in HEPES buffer (10 mM, pH 7.4) with 5% (v/v) DMSO, in the presence of BSA in a 1:1 ratio.

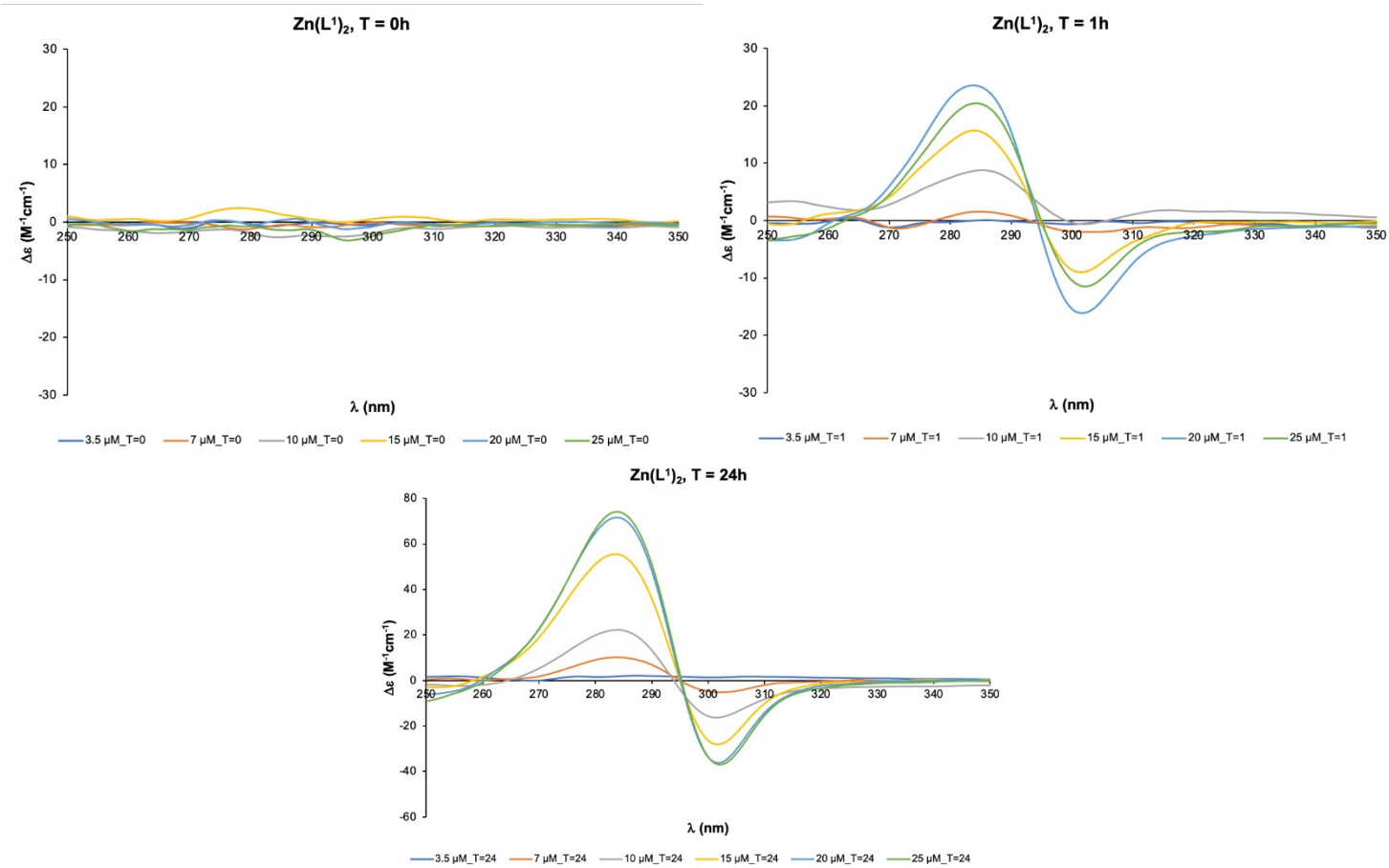

Figure S18. Changes of the CD spectra at different: BSA:**Zn(L^1)$_2$** ratios (1:0.35, 1:0.7, 1:1, 1:1.5, 1:2 and 1:2.5) at 0 h, 1 h and 24 h.

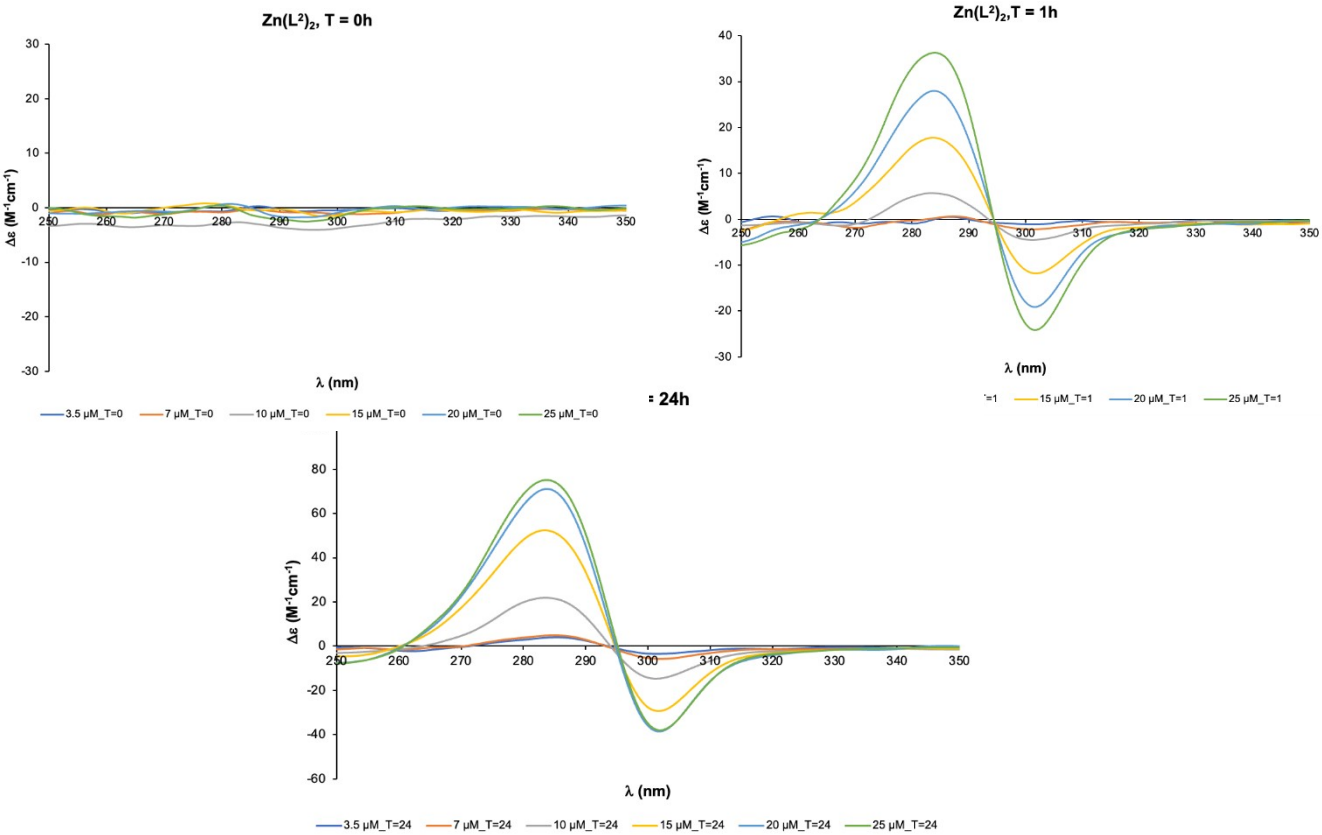

Figure S19. Changes of the CD spectra at different **$Zn(L^2)_2$** : BSA ratios (1:0.35, 1:0.7, 1:1, 1:1.5, 1:2 and 1:2.5) at 0 h, 1 h and 24 h.

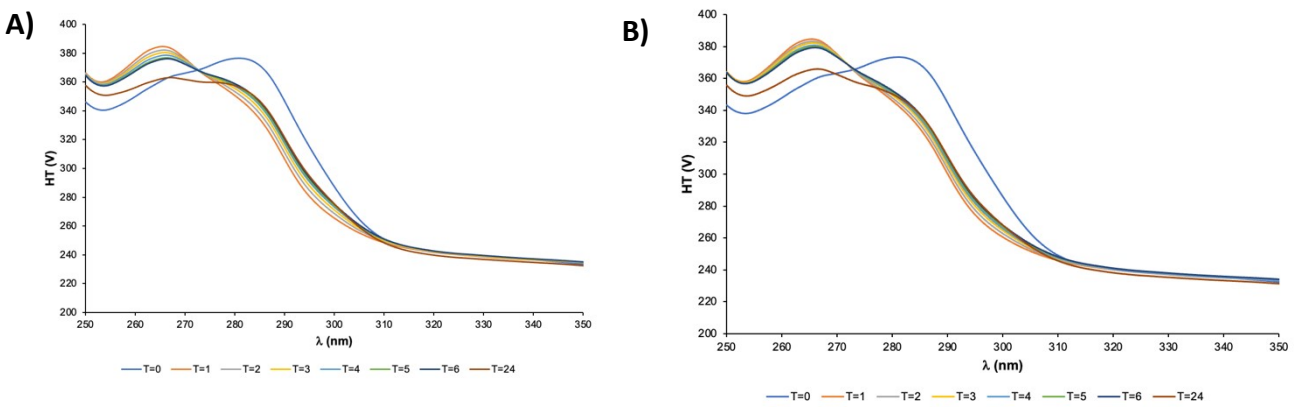

Figure S20. HT spectra of solutions containing BSA (10 μM) and **$Zn(L^1)_2$** – **A** or **$Zn(L^2)_2$** – **B** (1:2) measured with time (indicated in hours in the legend).

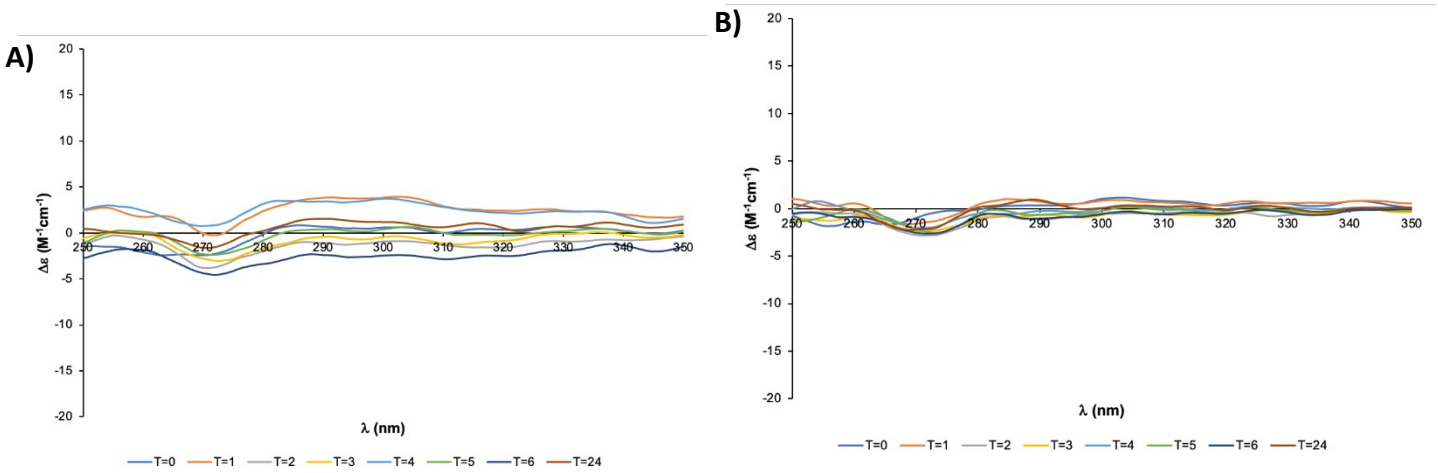

Figure S21. CD spectra of solutions containing BSA (10 μM) and **HL¹** – **A** or **HL²** – **B**(1:2) measured with time (indicated in hours in the legend).

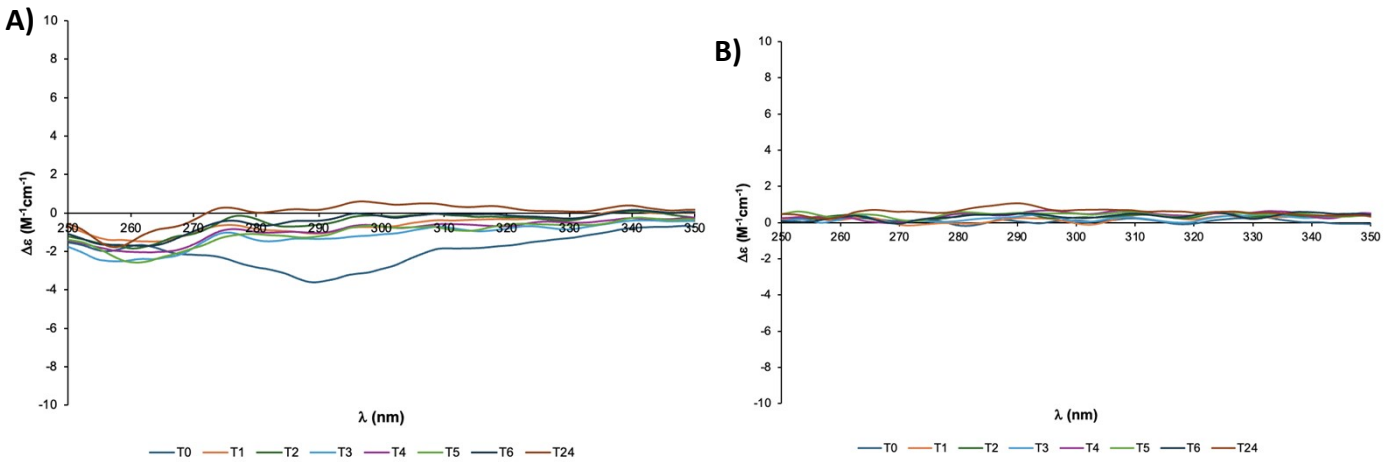

Figure S22. CD spectra of 20 μM solutions containing **$Zn(L^1)_2$** – **A** or **$Zn(L^2)_2$** – **B** in HEPES buffer measured with time (indicated in hours in the legend).

Table S8. Molecular docking [1, 2] to BSA (4OR0 molecule A with preserved original coordinates [3]): docking energies [kcal/mol] of the best fits for *R* - or *S* - warfarin, ibuprofen, the **HL^1** and **HL^2** ligands, and several isomers of the **Zn(L^1)$_2$** and **Zn(L^2)$_2$** complexes.

compound:	blind docking [a]	Trp213 box [b]	Trp134 box [c]
R - warfarin	-9.736	-9.533	-7.915
S - warfarin	-9.534	-10.230	-7.895
ibuprofen	-8.584	-8.016	-7.042
HL^1	-9.187	-9.182	-7.400
HL^2	-9.618	-9.641	-7.648
Zn(L^1)$_2$ - cc	-10.350	-8.289	-7.215
Zn(L^1)$_2$ - co	-10.120	-8.304	-7.204
Zn(L^1)$_2$ - oo	-9.795	-7.688	-7.280
Zn(L^1)$_2$ - oo - 180_flat square [d]	-9.743	-6.780	-7.706
Zn(L^1)$_2$ - oo - 180_distorted [d]	-9.385	-7.598	-7.491
Zn(L^2)$_2$ - cc	-10.700	-8.717	-7.629
Zn(L^2)$_2$ - co	-10.680	-8.689	-7.629
Zn(L^2)$_2$ - oo	-10.100	-8.236	-7.398
Zn(L^2)$_2$ - oo - 180_flat square [d]	-10.080	-7.320	-7.669
Zn(L^2)$_2$ - oo - 180_distorted [d]	-10.120	-8.334	-8.095

[a] best scores from the docking in the large boxes (74 x 64 x 86 Å^3 – 4 independent runs, and 91 x 60 x 75 Å^3 – 4 independent runs) centered at x = 8.830, y = 22.730, z = 99.460

[b] best scores from the Trp213 centered (x = -5.403, y = 22.893, z = 90.525) small boxes (25 x 25 x 25 Å^3 – 4 independent runs, and 30 x 30 x 30 Å^3 – 4 independent runs)

[c] best scores from the Trp134 centered (x = 19.535, y = 34.774, z = 90.525) small boxes (25 x 25 x 25 Å^3 – 4 independent runs, and 30 x 30 x 30 Å^3 – 4 independent runs)

[d] the **Zn(L^2)$_2$** - oo or **Zn(L^2)$_2$** - oo isomers with Γ (the C(8)-O-O-C(8) torsional angle – see **Fig. S11**) = 180°

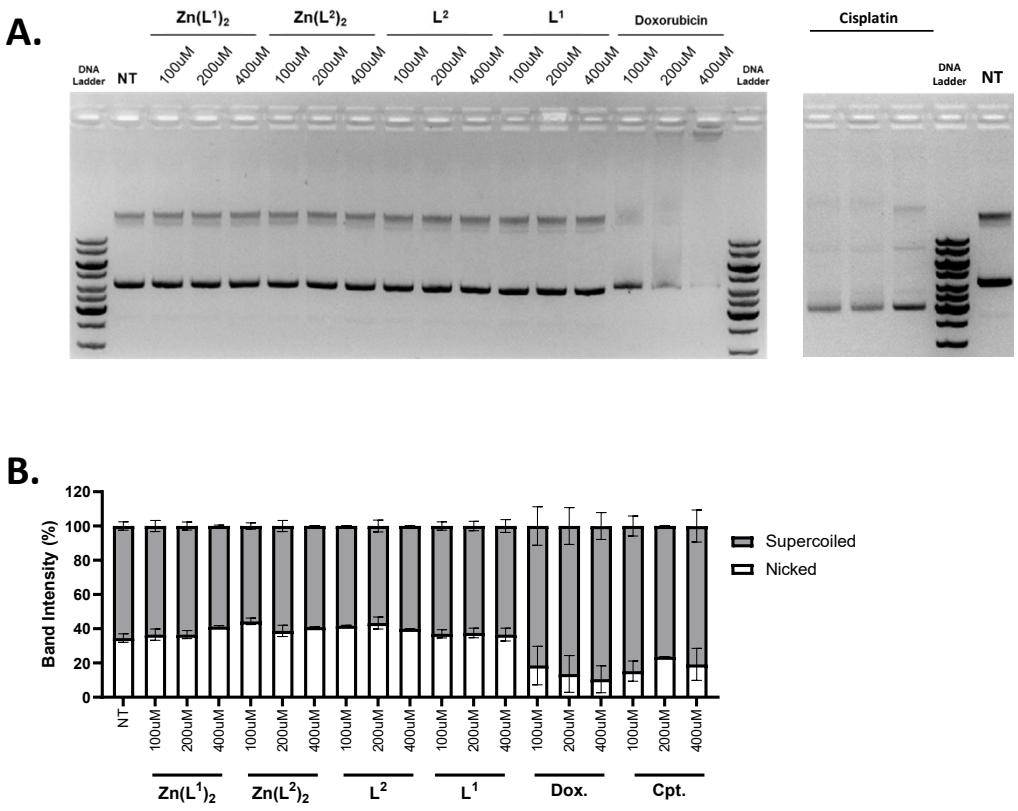

Figure S23. Gel electrophoresis of plasmid DNA treated with compounds **$Zn(L^1)_2$**, **$Zn(L^2)_2$**, **HL^2**, **HL^1**. Doxorubicin (Dox.) and Cisplatin (Cpt.) were used as positive control. Plasmid DNA was incubated with different concentrations of compounds (100, 200 and 400 μM) overnight at room temperature. The intensity of the bands in each lane was quantified and represented as mean ± standard error of the mean (SEM). (**A**) Representative gel images (**B**) Quantitative assessment of band intensities.

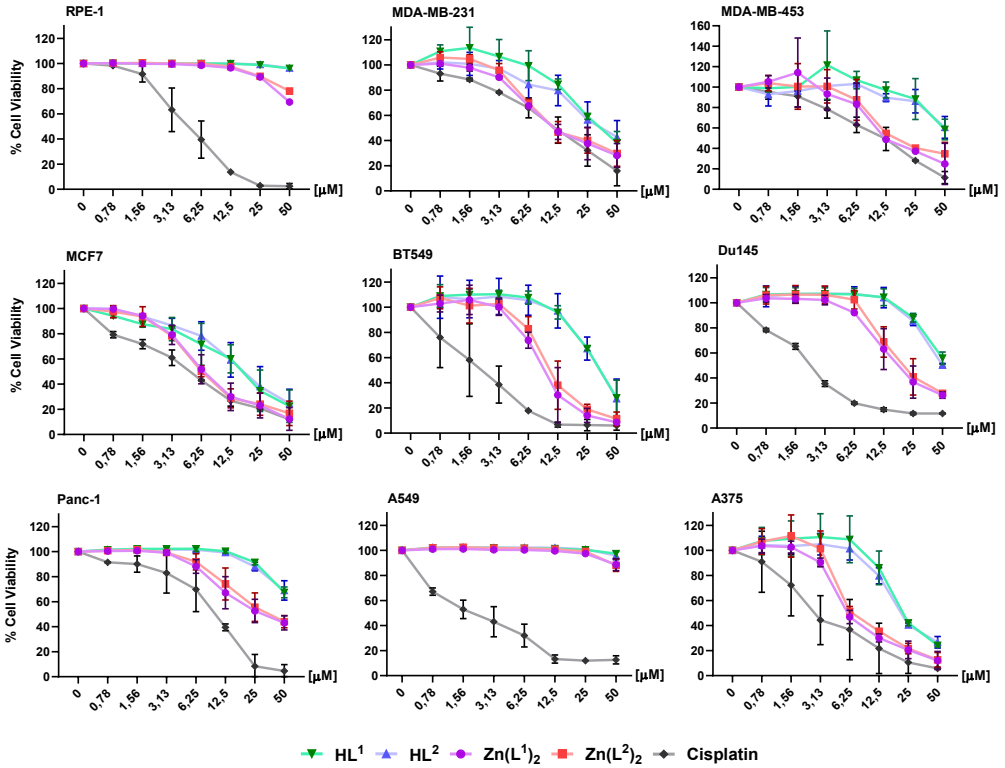

Figure S24. Cell viability results as determined by *Sulforhodamine B (SRB) assay:* RPE-1, MDA-MB-231, MDA-MB-453, MCF7, BT549, Du145, Panc-1, A549 and A375 cells were exposed to compounds for 72 h. Error bars represent the standard deviation from the mean.

References

[1] O. Trott, A.J. Olson, Software News and Update AutoDock Vina: Improving the Speed and Accuracy of Docking with a New Scoring Function, Efficient Optimization, and Multithreading, J. Comput. Chem., 31 (2010) 455-461.
[2] J. Eberhardt, D. Santos-Martins, A.F. Tillack, S. Forli, AutoDock Vina 1.2.0: New Docking Methods, Expanded Force Field, and Python Bindings, J. Chem. Inf. Model., 61 (2021) 3891-3898.
[3] A. Bujacz, K. Zielinski, B. Sekula, Strucural studies of bovine, equine, and leporine serum albumin complexes with naproxen, Proteins, 82 (2014) 2199-2208.